Space–Time Block-Coded Multiple Access Through Frequency-Selective Fading Channels

Zhiqiang Liu and Georgios B. Giannakis, *Fellow, IEEE*

***Abstract*—Mitigation of multipath fading effects and suppression of multiuser interference (MUI) constitute major challenges in the design of wide-band third-generation wireless mobile systems. Space–time (ST) coding offers an effective transmit-antenna diversity technique to combat fading, but most existing ST coding schemes assume flat fading channels that may not be valid for wide-band communications. Single-user ST coded orthogonal frequency-division multiplexing transmissions over frequency-selective channels suffer from finite-impulse response channel nulls (fades). Especially multiuser ST block-coded transmissions through (perhaps unknown) multipath present unique challenges in suppressing not only MUI but also intersymbol/chip interference. In this paper, we design ST multiuser transceivers suitable for coping with frequency-selective multipath channels (downlink or uplink). Relying on symbol blocking and a single-receive antenna, ST block codes are derived and MUI is eliminated without destroying the orthogonality of ST block codes. The system is shown capable of providing transmit diversity while guaranteeing symbol recovery in multiuser environments, regardless of unknown multipath. Unlike existing approaches, the mobile does not need to know the channel of other users. In addition to decoding simplicity, analytic evaluation and corroborating simulations reveal its flexibility and performance merits.**

***Index Terms*—Dispersive channels, diversity methods, multiuser detection, ST codes, transmit antennas.**

I. Introduction

THE UPCOMING growth in demand for high-capacity data rates and new services necessitates the development of wide-band wireless systems. In the design of such systems, two critical performance and capacity limiting factors are multipath fading and multiuser interference (MUI).

Transmit diversity has been studied extensively for combating fading and improving capacity (see [9] and [12] and references therein). Specifically, transmit diversity schemes based on space–time (ST) coding exploit multiple transmissions that are combined with appropriate signal processing at the receiver to provide diversity gain. ST trellis codes were first proposed in [18] to achieve maximum diversity gain at the expense of increased complexity of optimal decoding at the receiver. To reduce decoding complexity, suboptimal approaches have been developed including multistage decoding [18] and antenna partitioning [17]. ST *block* coding emerged as an attractive alternative because it leads to maximum-likelihood (ML) decoding using only linear receiver processing [2], [15].

ST codes were originally designed for *single-user* systems and investigated for known slow *flat fading* channels [16]–[18]. Unlike narrow-band transmissions, the flat-fading channel assumption is no longer justified in wide-band communications, which motivated recent extensions of ST coding to *frequency-selective* channels for orthogonal frequency-division multiplexing (OFDM) [1], [5] and generalized OFDM (GOFDM) systems [8], [21]. With transmit diversity, ST coded (G)OFDM can ameliorate (but not eliminate) fading effects caused by channel nulls (fades). However, when transmit antennas are not well separated, the multiple channels become correlated, and symbol recovery is not assured because nulls common to the multiple channels are possible to occur. Different from [1] and [5], the so-called "root-rotating" variant of [8] and [21] avoids persistent deep fading caused by common channel nulls and improves the overall system performance; but symbol recovery is still not guaranteed.

ST coding for *multiuser* systems is challenging due to the presence of severe MUI. For an M-user system where each user is equipped with N_t transmit antennas, MUI is caused by $(M-1)N_t$ instead of $M-1$ interfering signals. Assuming flat fading channels, [11] exploited the structure of ST block codes to suppress MUI in space using a beamforming approach that relies on multiple receive antennas. To cancel MUI however, a minimum of M receive antennas is required, which limits practicality especially in the downlink where the receiver complexity is at a premium. Furthermore, the per-user performance of [11] relative to the single-user system in [2] and [15] may suffer after the beamforming-based suppression of MUI.

In this paper, we develop novel ST multiuser transceivers for multiple access through frequency-selective channels. Each user is equipped with multiple transmit antennas, but only one receive antenna will be sufficient. Our system design and goal is threefold. First, we adopt and extend the generalized multicarrier code-division multiple-access (GMC-CDMA) design of [4] and [19] to our ST context. By judicious design of users' spreading codes, MUI from all transmit antennas of interfering users is eliminated deterministically regardless of the finite-impulse response (FIR) channels encountered. Having eliminated MUI, we then rely on symbol blocking and develop novel ST block coders (counterparts of [15]) to achieve transmit diversity gain. To guarantee symbol recovery regardless of channel nulls, we capitalize on *redundant transmit precoding*. The resulting system retains the simplicity and performance of a single-user system [2], [15] even with multiple-access

Paper approved by A. Goldsmith, the Editor for Wireless Communication of the IEEE Communications Society. Manuscript received November 15, 1999; revised November 15, 2000. This work was supported by the ARO under Grant DAAG55-98-1-0336. This paper was presented in part at the First Sensor Array and Multichannel Signal Processing Workshop, Boston, MA, March 15–17, 2000.

The authors are with the Department of Electrical and Computer Engineering, University of Minnesota, Minneapolis, MN 55455 USA (e-mail: lzq@ece.umn.edu; georgios@ece.umn.edu).

Publisher Item Identifier S 0090-6778(01)04865-6.

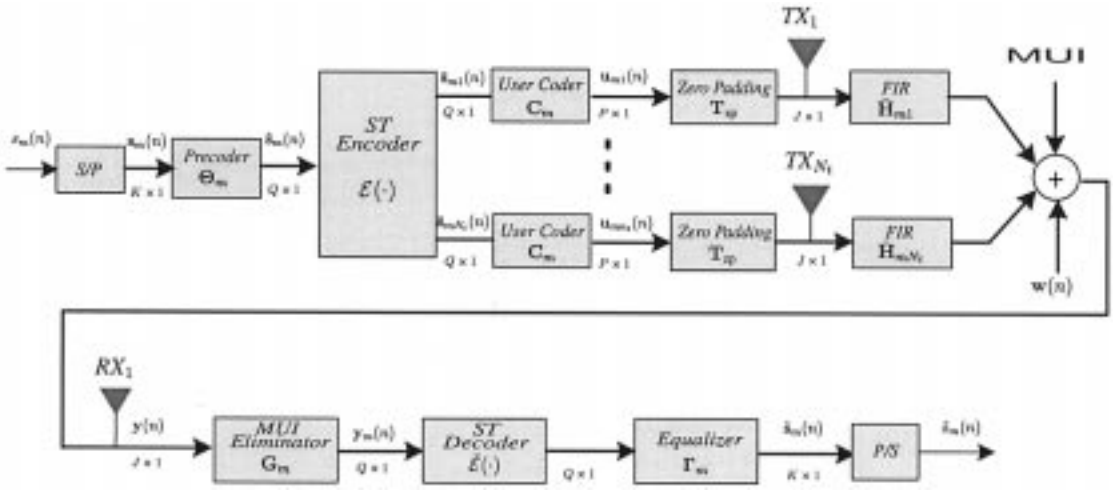

Fig. 1. Discrete-time equivalent baseband system model for the mth user.

communications over frequency-selective channels. Unlike [11] where channel knowledge of all users is needed and multiple antennas are required at the receiver, the proposed system needs to know the channels of the desired user only and is applicable even with a single receive antenna, which greatly reduces the receiver complexity. It also relieves the burden of channel estimation, timing acquisition, and synchronization, which are very attractive features especially for the downlink.

The paper is organized as follows. In Section II, we describe the system model. In Section III, we design users' spreading codes for deterministic MUI elimination. ST coding and symbol recovery designs are presented in Section IV. Some important design issues are addressed in Section V. Bit-error rate (BER) performance is analyzed and corroborating simulations are presented in Section VI. Section VII concludes this paper.

Notation: Column vectors (matrices) are denoted by boldface lower (upper) case letters. Superscripts $T, *, \mathcal{H}, \dagger$ stand for transpose, complex conjugate, complex conjugate transpose, and matrix pseudoinverse, respectively; $\mathrm{diag}(d_1, \ldots, d_M)$ denotes an $M \times M$ diagonal matrix with diagonal entries $d_1, \ldots, d_M$, $\mathbf{0}_{M\times N}$ denotes the $M \times N$ matrix with all zero entries, and $\mathbf{I}_M$ the $M \times M$ identity matrix. Matlab notation $\mathbf{A}(:, n)$ is used for the nth column of matrix $\mathbf{A}$.

II. Modeling and Problem Statement

Fig. 1 depicts the discrete-time equivalent baseband model of a chip-sampled quasi-synchronous (QS) multiuser communication system (as in [3] and [19]) with N_t transmit antennas and a single receive antenna for each user (only transmitter, channel, and receiver for one user, the mth, are shown). Each of the M users transmits the information sequence $s_m(n)$ in blocks $\mathbf{s}_m(n) := [s_m(nK), \ldots, s_m(nK + K - 1)]^T$ of size $K \times 1$. The filterbank described by the tall $Q \times K$ matrix $\mathbf{\Theta}_m$, with generally complex entries, constitutes our redundant ($Q > K$) precoder that will facilitate symbol recovery. The $Q \times 1$ precoded blocks

$$\tilde{\mathbf{s}}_m(n) := [\tilde{s}_m(nQ), \ldots, \tilde{s}_m(nQ + Q - 1)]^T = \mathbf{\Theta}_m \mathbf{s}_m(n) \tag{1}$$

are fed into the ST encoder $\mathcal{E}(\cdot)$. The ST encoder takes N_s consecutively precoded blocks $\tilde{\mathbf{s}}_m(n)$, which we denote by $\check{\mathbf{s}}_m(i) := [\tilde{\mathbf{s}}_m^T(iN_s), \ldots, \tilde{\mathbf{s}}_m^T(iN_s + N_s - 1)]^T$, to output the following $N_d Q \times N_t$ matrix of ST encoded blocks:

$$\overline{\mathbf{S}}_m(i) = \mathcal{E}(\check{\mathbf{s}}_m(i)) = \begin{bmatrix} \overline{\mathbf{s}}_{m1}(iN_d) & \cdots & \overline{\mathbf{s}}_{mN_t}(iN_d) \\ \vdots & \ddots & \vdots \\ \overline{\mathbf{s}}_{m1}(iN_d + N_d - 1) & \cdots & \overline{\mathbf{s}}_{mN_t}(iN_d + N_d - 1) \end{bmatrix} \tag{2}$$

whose rows are generated in successive time intervals with each of the N_t blocks in a given row forwarded to one of the N_t transmit antennas. For convenience, we denote $\overline{\mathbf{s}}_{mn_t}(n) := [\overline{s}_{mn_t}(nQ), \ldots, \overline{s}_{mn_t}(nQ + Q - 1)]^T$ the $Q \times 1$ block transmitted through the n_t transmit-antenna at the time n. The link between the ST encoded output block $\overline{\mathbf{s}}_{mn_t}(n)$ and the precoded input block $\tilde{\mathbf{s}}_m(n)$ will offer the desirable transmit diversity gain as we will detail in Section IV. Before transmission, each user's spreading code described by the $P \times Q$ matrix $\mathbf{C}_m$ is applied to $\overline{\mathbf{s}}_{mn_t}(n)$ to produce the block $\mathbf{u}_{mn_t}(n) := \mathbf{C}_m \overline{\mathbf{s}}_{mn_t}(n)$ of length $P > Q$. Each user's spreading code matrix $\mathbf{C}_m$ will be designed to eliminate the MUI in Section III.

After parallel-to-serial (P/S) conversion (not shown in Fig. 1), the P-long block $\mathbf{u}_{mn_t}(n)$ propagates through the Lth-order discrete-time baseband equivalent FIR channel $\{h_{mn_t}(l)\}_{l=0}^{L}$. The channel includes transmit–receive pulse-shaping filters, multipath, and quasi-synchronism among users.[1] We underscore that except for an upper bound L on the maximum channel order that is assumed available, we do not need to

[1]In QS systems, every user tries to synchronize with the base station's pilot signal. Therefore, users are not totally asynchronous but they are allowed to be off by a few chips accounting for relative delay and timing errors. Such a bounded asynchronism is captured by pure delay FIR filters in our model. With $\tau_{\max,\,d}$ denoting the channels' maximum delay spread and $\tau_{\max,\,a}$ denoting the maximum relative asynchronism among users, the upper bound of the channel order is $L = \lceil (\tau_{\max,\,d} + \tau_{\max,\,a})/T_c \rceil$ where sampling at the chip rate $1/T_c$ is assumed at the receive-filter's output and $\lceil \cdot \rceil$ stands for integer-ceiling. Of course, $\tau_{\max,\,a} = 0$ in the downlink.

know the channels $\{h_{mn_t}(l)\}_{n_t=1}^{N_t}$ at the transmitter. In order to eliminate the interblock interference (IBI) caused by the FIR channels, we pad L zero symbols at the end of $\mathbf{u}_{mn_t}(n)$, which can be described by the product $\mathbf{T}_{zp}\mathbf{u}_{mn_t}(n)$ where the $J \times P$ matrix $\mathbf{T}_{zp} := [\mathbf{I}_P^T \mathbf{0}_{L\times P}^T]^T$ and $J := P + L$. Padding L guard zeros reduces bandwidth efficiency, but this reduction can be made arbitrarily small by increasing the block size K, as we will discuss in Section V. Zero-padding (ZP) is an alternative to the cyclic prefix (CP) that is introduced at OFDM transmitters and is discarded at OFDM receivers to remove IBI [6] (see also [10], [22], and [19] for comparisons between ZP and CP). The FIR channel operation on the transmitted data is described by the $J \times J$ Toeplitz matrix $\overline{\mathbf{H}}_{mn_t}$ with first row $[h_{mn_t}(0)\mathbf{0}_{1\times(J-1)}]$ and first column $[h_{mn_t}(0)\cdots h_{mn_t}(L)\mathbf{0}_{1\times(J-L+1)}]^T$, as shown in Fig. 1.

After serial-to-parallel (S/P) conversion (not shown in Fig. 1), the nth received IBI-free block $\mathbf{y}(n) := [y(nJ), \ldots, y(nJ + J - 1)]^T$ from all M users is given by

$$\mathbf{y}(n) = \mathbf{x}_m(n) + \sum_{\mu=0,\,\mu\neq m}^{M-1} \mathbf{x}_\mu(n) + \mathbf{w}(n) \tag{3}$$

where $\mathbf{w}(n) := [w(nJ), \ldots, w(nJ + J - 1)]^T$ denotes additive white Gaussian noise (AWGN). $\mathbf{x}_m(n) := [x_m(nJ), \ldots, x_m(nJ + J - 1)]^T$ is the noise-free received block from the mth user that is expressed as

$$\mathbf{x}_m(n) = A_m \sum_{n_t=1}^{N_t} \mathbf{H}_{mn_t}\mathbf{C}_m\bar{\mathbf{s}}_{mn_t}(n) \tag{4}$$

where $\mathbf{H}_{mn_t} := \overline{\mathbf{H}}_{mn_t}\mathbf{T}_{zp}$ is a Toeplitz channel matrix of size $J \times P$ and A_m is the mth user's amplitude. The vector $\mathbf{y}(n)$ in (3) consists of three terms: the first term is useful information from the desired (here the mth) user, the second term is MUI, and the third term is additive receiver noise.

Given the received block $\mathbf{y}(n)$, the recovery of $\mathbf{s}_m(n)$ will be sought in three steps. First, $\mathbf{y}(n)$ will be filtered by the user-separating filter described by the $Q \times J$ matrix $\mathbf{G}_m$ to eliminate MUI. Second, the MUI-free $\mathbf{y}_m(n)$ will be processed by the ST decoder $\overline{\mathcal{E}}(\cdot)$ to collect the embedded transmit diversity built by the ST encoder (see Fig. 1). Finally, a low-complexity block linear equalizer described by the $K \times J$ matrix $\mathbf{\Gamma}_m$ will be used to eliminate ISI and recover $\mathbf{s}_m(n)$. Accordingly, the goal of our system *design* includes the following three *stages*.

d1) *MUI Elimination Stage:* Consists of designing the users' spreading code matrices $\mathbf{C}_m$ and their separating filters $\mathbf{G}_m$, and selecting their dimensions to guarantee deterministic MUI elimination regardless of the underlying FIR channels, the chosen signal constellation, and with minimum redundancy.

d2) *ST Encoding/Decoding Stage:* Consists of designing the ST encoder $\mathcal{E}(\cdot)$ and decoder $\overline{\mathcal{E}}(\cdot)$, and selecting the parameters N_s, N_d, N_t, to achieve transmit diversity gain regardless of the underlying FIR channels, the chosen signal constellation, and with minimum redundancy.

d3) *Symbol Recovery Stage:* consists of designing the precoder $\mathbf{\Theta}_m$ and the equalizer $\mathbf{\Gamma}_m$, and selecting the block sizes K and Q to guarantee symbol recovery regardless of the FIR channel nulls, the signal constellation, and with minimum redundancy.

III. User Codes for Deterministic MUI Elimination

Due to the multi-antenna transmissions, the MUI in (3) consists of $(M-1)N_t$ interfering signals instead of $M-1$ as in [4] and [19]. Observe though that the same spreading code is chosen for the N_t transmit-antenna branches of each user. Accordingly, the $(M-1)N_t$ interfering signals in (3) can be partitioned into $M-1$ groups with respect to their spreading codes. Our basic idea to eliminate the MUI is to adopt the user-separating capability of the single transmit- and receive-antenna GMC-CDMA design [4], [19] and extend it to our ST context. As in [4] and [19], we will design jointly the users' spreading codes $\{\mathbf{C}_\mu\}_{\mu=0}^{M-1}$ and their separating filters $\{\mathbf{G}_\mu\}_{\mu=0}^{M-1}$ to eliminate the MUI deterministically, *regardless* of the underlying FIR channels, the chosen constellation, and with minimum redundancy.

Let us first choose $P = MQ$ and define the set $\mathcal{P} := \{\rho_0, \ldots, \rho_{P-1}\}$ where ρ_ps are P *distinct* points on the complex plane. We term here the set $\mathcal{P}$ as our signature set and its members (ρ_ps) as signature points.[2] With a total of P signature points, the μth user is allocated Q signature points $\{\rho_{\mu,q}\}_{q=1}^{Q-1}$ (where $\rho_{\mu,q} \in \mathcal{P}$) and different users have different signature points. Let the set $\mathcal{I} := \{1, 2, \ldots, P\}$ be indexing the collection of all signature points in $\mathcal{P}$. Mathematically, the allocation of signature points can be represented by partitioning the set $\mathcal{I}$ into M nonintersecting subsets $\mathcal{I}_\mu$, i.e.,

$$\bigcup_{\mu=0}^{M-1} \mathcal{I}_\mu = \mathcal{I} \quad \mathcal{I}_\mu \bigcap \mathcal{I}_m = \emptyset \qquad \forall\, \mu \neq m \tag{5}$$

where $\emptyset$ denotes the empty set and the subset $\mathcal{I}_\mu$ collects the indeces of $\{\rho_{\mu,q}\}_{q=1}^{Q-1}$ in the set $\mathcal{P}$. To link $\mathcal{I}_\mu$ with the operation of signature point allocation, we further define for the μth user the signature selector matrix $\mathbf{\Phi}_\mu = \mathbf{I}_P(:, \mathcal{I}_\mu)$, where $\mathbf{I}_P(:, \mathcal{I}_\mu)$ is a $P \times Q$ permutation matrix built from the $\mathcal{I}_\mu$ columns of the $P \times P$ identity matrix $\mathbf{I}_P$. Because permutation matrices have orthogonal columns, it follows that the signature selector matrices are orthogonal to each other, i.e.,

$$\mathbf{\Phi}_\mu^T\mathbf{\Phi}_m = \delta(\mu - m)\mathbf{I}_Q \tag{6}$$

where $\delta(\cdot)$ denotes Kronecker's delta. The orthogonality (6) will be exploited for MUI elimination.

[2]Relying on a $\mathcal{Z}$-transform approach, the MUI-free $\{\mathbf{C}_m, \mathbf{G}_m\}$ transceivers of this section were derived originally in [4] and for the ST context in the conference precursor of this paper [7]. For signature points chosen on the fast Fourier transform (FFT) grid, the matrix formulation of this section was introduced in [19]. Such equispaced points in [19] correspond to taking the inverse FFT twice, which amounts to time-reversing transmitted blocks, and transmitting them with single-carrier modulation [24]; i.e., our original solution in [19] covers both single- and multicarrier schemes, but here we will focus on the latter.

Before we proceed, let us first build from the set $\mathcal{P}$ the following two Vandermonde matrices as:

$$\mathcal{V}_1 := \begin{bmatrix} 1 & \rho_0^{-1} & \cdots & \rho_0^{-(P-1)} \\ 1 & \rho_1^{-1} & \cdots & \rho_1^{-(P-1)} \\ \vdots & \vdots & & \vdots \\ 1 & \rho_{P-1}^{-1} & \cdots & \rho_{P-1}^{-(P-1)} \end{bmatrix}_{P\times P}$$

$$\mathcal{V}_2 := \begin{bmatrix} 1 & \rho_0^{-1} & \cdots & \rho_0^{-(J-1)} \\ 1 & \rho_1^{-1} & \cdots & \rho_1^{-(J-1)} \\ \vdots & \vdots & & \vdots \\ 1 & \rho_{P-1}^{-1} & \cdots & \rho_{P-1}^{-(J-1)} \end{bmatrix}_{P\times J}. \quad (7)$$

Recalling that $\{\rho_p\}_{p=0}^{P-1}$ were chosen to be distinct, we deduce that the matrix $\mathcal{V}_1$ is full rank, i.e., its inverse $\mathcal{V}_1^{-1}$ always exists. The μth user's spreading code matrix $\mathbf{C}_\mu$ and corresponding separating filter $\mathbf{G}_\mu$ are designed as

$$\mathbf{C}_\mu = \mathcal{V}_1^{-1}\mathbf{\Phi}_\mu, \quad \mathbf{G}_\mu = \mathbf{\Phi}_\mu^T\mathcal{V}_2, \qquad \mu = 0, \ldots, M-1. \quad (8)$$

If ρs in (7) are chosen equispaced on the unit circle (FFT grid), then $(\mathcal{V}_1^{-1})\mathcal{V}_2$ correspond to (I)FFT matrices and the selectors $\mathbf{\Phi}_\mu$ in (8) allocate distinct user-specific subcarriers. Substituting (8) into (4), we obtain from (3) the receiver filter output $\mathbf{y}_m(n) := \mathbf{G}_m\mathbf{y}(n)$ as follows (see also Fig. 1):

$$\begin{aligned}\mathbf{y}_m(n) = A_m &\sum_{n_t=1}^{N_t} \mathbf{\Phi}_m^T\mathcal{V}_2\mathbf{H}_{mn_t}\mathcal{V}_1^{-1}\mathbf{\Phi}_m\bar{\mathbf{s}}_{mn_t}(n) \\ &+ \sum_{\mu=0,\,\mu\neq m}^{M-1} A_\mu \sum_{n_t=1}^{N_t} \mathbf{\Phi}_m^T\mathcal{V}_2\mathbf{H}_{\mu n_t}\mathcal{V}_1^{-1}\mathbf{\Phi}_\mu\bar{\mathbf{s}}_{\mu n_t}(n) \\ &+ \mathbf{\Phi}_m^T\mathcal{V}_2\mathbf{w}(n). \end{aligned} \quad (9)$$

To eliminate the MUI [the second sum in the right-hand side of (9)], we rely on the following two facts that can be proved easily by direct substitution.

Fact 1: The Toeplitz channel matrix $\mathbf{H}_{\mu n_t}$ is diagonalized by performing $\mathcal{V}_2\mathbf{H}_{\mu n_t}\mathcal{V}_1^{-1}$, i.e.,

$$\mathcal{V}_2\mathbf{H}_{\mu n_t}\mathcal{V}_1^{-1} = \mathbf{D}_{H_{\mu n_t}} := \mathrm{diag}[H_{\mu n_t}(\rho_0), \ldots, H_{\mu n_t}(\rho_{P-1})]$$

where $H_{\mu n_t}(\rho_p) := \sum_{l=0}^{L} h_{\mu n_t}(l)\rho_p^{-l}$ is the $\mathcal{Z}$-transform of the channel $h_{\mu n_t}(l)$ evaluated at the signature point ρ_p. For circulant channel matrices that are created when CP is used instead of ZP, Fact 1 amounts to their diagonalization via (I)FFT matrices (see, e.g., [19]).

Fact 2: Denoting $\mathcal{D}_{\mu n_t} := \mathbf{\Phi}_\mu^T\mathbf{D}_{H_{\mu n_t}}\mathbf{\Phi}_\mu = \mathrm{diag}[H_{\mu n_t}(\rho_{\mu,0}), \ldots, H_{\mu n_t}(\rho_{\mu,Q-1})]$, it holds true that

$$\mathbf{D}_{H_{\mu n_t}}\mathbf{\Phi}_\mu = \mathbf{\Phi}_\mu\mathcal{D}_{\mu n_t}.$$

Fact 2 simply states that with appropriate changes in dimensionalities, diagonal matrices commute with permutation matrices.

Exploiting the Facts 1) and 2) along with the orthogonality of (6), the user separating filter output $\mathbf{y}_m(n)$ in (9) can be rewritten as

$$\begin{aligned}\mathbf{y}_m(n) &= A_m \sum_{n_t=1}^{N_t} \mathbf{\Phi}_m^T\mathcal{V}_2\mathbf{H}_{mn_t}\mathcal{V}_1^{-1}\mathbf{\Phi}_m\bar{\mathbf{s}}_{mn_t}(n) \\ &\quad + \mathbf{\Phi}_m^T\mathcal{V}_2\mathbf{w}(n) \\ &= A_m \sum_{n_t=1}^{N_t} \mathcal{D}_{mn_t}\bar{\mathbf{s}}_{mn_t}(n) + \boldsymbol{\eta}_m(n) \end{aligned} \quad (10)$$

where $\boldsymbol{\eta}_m(n) := \mathbf{\Phi}_m^T\mathcal{V}_2\mathbf{w}(n)$ denotes the residual noise. It is clear from (10) that the MUI has been eliminated deterministically through the mutually orthogonal designs of $\mathbf{C}_\mu$ and $\mathbf{G}_\mu$ in (8). Note that the MUI elimination here is achieved *without* requiring channel state information (CSI) at the receiver. Observe also that the equivalent channel matrix $\mathcal{D}_{mn_t}$ is diagonal instead of the Toeplitz convolution matrix $\mathbf{H}_{mn_t}$ that corresponds to our frequency-selective channels in (4). We infer that our MUI elimination has also converted each frequency-selective channel into a set of frequency-flat subchannels. The diagonal structure of $\mathcal{D}_{mn_t}$ will be exploited in the next section to develop our ST block codes.

We now summarize our deterministic MUI elimination design as follows.

- d1.1) Choose $P = MQ$ and $J = P + L$.
- d1.2) Select P distinct complex points $\{\rho_p\}_{p=0}^{P-1}$ and assign them to disjoint subsets $\{\mathcal{I}_\mu\}_{\mu=0}^{M-1}$.
- d1.3) Set up the users' spreading codes $\mathbf{C}_\mu$ and their separating filters $\mathbf{G}_\mu$ according to (8).

Having eliminated MUI, we proceed next to design ST block encoders/decoders that collect transmit diversity gains.

IV. Space–Time Block Coding and Symbol Recovery

One advantage of the MUI-free transceivers is that multiple users can be separated by design and each user can be viewed as transmitting through his/her own multiple-antenna channels. Consequently, ST coding design for a multiuser system has been converted into an equivalent set of single-user systems, which greatly reduces the receiver complexity per user. Without loss of generality, we will focus on the mth user and start with the MUI-free received data model in (10). We wish to design the ST encoder $\mathcal{E}(\cdot)$ and decoder $\overline{\mathcal{E}}(\cdot)$ to recover $\mathbf{s}_m(n)$ from $\mathbf{y}_m(n)$ with transmit diversity gain. For the moment, we suppose that $\{\mathcal{D}_{mn_t}\}_{n_t=1}^{N_t}$ [or equivalently the channels $h_{mn_t}(l)$] are known at the receiver. We underscore that the mth user's receiver does not need to know the channels from all interfering users and only has to estimate his/her own channels, i.e., $h_{mn_t}(l)$. The issue of (even blind) channel estimation in our system will be discussed later.

The design of ST block codes was cast as a generalized complex orthogonal design (GCOD) problem in [15], for single-user symbol-by-symbol transmissions over flat fading channels. The orthogonal structure of ST block codes leads to low-complexity ML decoding. However, as indicated in (3), we deal in our system with block-by-block transmissions through frequency-selective channels where code orthogonality

is generally destroyed. Recall from (10) that MUI elimination has converted each frequency-selective channel to a set of flat subchannels. Our basic objective is to achieve transmit diversity through these flat subchannels by developing a novel counterpart of GCOD which is suitable for block transmissions. Note that the generalized real orthogonal designs of [15] are not applicable here because the equivalent channels $\mathcal{D}_{mn_t}$ could be complex valued even when real constellations are used.

A. GCOD

Details for GCOD can be found in [15], but for the reader's convenience in introducing notation, we will briefly review GCOD, starting with the following definition.

Definition 4.1 [15]: Define the $L_s \times 1$ vector $\mathbf{s} := [s_0, \ldots, s_{L_s-1}]^T$ and let $\mathcal{O}(\mathbf{s})$ be an $L_d \times N_t$ matrix with entries $0, \pm s_0, \pm s_0^*, \ldots, \pm s_{L_s-1}, \pm s_{L_s-1}^*$, or their linear combinations. If $\mathcal{O}^{\mathcal{H}}(\mathbf{s})\mathcal{O}(\mathbf{s}) = \alpha(|s_0|^2 + \cdots + |s_{L_s-1}|^2)\mathbf{I}_{N_t}$ for some positive constant α, then $\mathcal{O}(\mathbf{s})$ is termed a GCOD in variables $s_0, \ldots, s_{L_s-1}$ of size $L_d \times N_t$ and rate $R = L_s/L_d$.

A GCOD of size $L_d \times N_t$ is designed to achieve transmit diversity gain of order N_t for a system with N_t transmit antennas [15]. For a fixed number of transmit antennas, one is interested in GCOD's with maximum rate R that are spectrally most efficient. On the existence of GCOD's, we know from [15] the following:

i) for $N_t = 2$, a GCOD with maximum rate $R = 1$ exists;
ii) for $N_t = 3, 4$, GCOD's exist but with rate $R = 3/4$;
iii) for $N_t > 4$, GCOD's exist with rate $R = 0.5$.

As an example of GCOD for $N_t = 2$, one reaches the design of [2]

$$\mathcal{O}_2 = \begin{bmatrix} s_0 & s_1 \\ -s_1^* & s_0^* \end{bmatrix}. \tag{11}$$

Whether GCOD's with rates higher than those in ii) and iii) exist is an open question. But here we will adopt the GCOD's of [15] and focus on extending them to our system described in Section II.

B. Block ST Encoder Design

ST encoder design in our system depends on the selection of the parameters N_t, N_s, and N_d (see Section II). The choice of N_t (the number of transmit antennas) is mainly dictated by complexity, size, and cost considerations at the transmitter. For a given N_t, choosing N_s and N_d starts with looking for an available GCOD, call it $\mathcal{O}_{N_t}$, of size $L_d \times N_t$ with maximum rate R, if possible. Then N_d and N_s are chosen as $N_d = L_d$ and $N_s = L_s = RL_d$. Based on GCOD's i)–iii) of the previous subsection, the selection of (N_s, N_d) is listed as follows:

$$(N_s, N_d) = \begin{cases} (2, 2), & \text{if } N_t = 2 \\ (3, 4), & \text{if } N_t = 3, 4 \\ (N_t, 2N_t), & \text{if } N_t > 4. \end{cases} \tag{12}$$

Suppose that the selected $\mathcal{O}_{N_t}$ is an $N_d \times N_t$ GCOD in variables $s_0, \ldots, s_{N_s-1}$. We proceed to design our ST encoder $\mathcal{E}(\cdot)$ by first representing $\mathcal{O}_{N_t}$ as [15]

$$\mathcal{O}_{N_t} = \sum_{n_s=0}^{N_s-1} \left(\mathbf{A}_{n_s} s_{n_s} + \mathbf{B}_{n_s} s_{n_s}^*\right) \tag{13}$$

where $\mathbf{A}_{n_s}$ and $\mathbf{B}_{n_s}$ are $N_d \times N_t$ *real* matrices which are uniquely determined by $\mathcal{O}_{N_t}$ (cf. Definition 4.1).

Our novel ST encoder $\mathcal{E}(\cdot)$ is constructed as the *block* counterpart of $\mathcal{O}_{N_t}$ in (13). Specifically, using the matrix pairs $\{\mathbf{A}_{n_s}, \mathbf{B}_{n_s}\}_{n_s=0}^{N_s-1}$, the matrix $\overline{\mathbf{S}}_m(i)$ in (2) that defines our block GCOD is specified as

$$\overline{\mathbf{S}}_m(i) = \sum_{n_s=0}^{N_s-1} [\mathbf{A}_{n_s} \otimes \tilde{\mathbf{s}}_m(iN_s+n_s) + \mathbf{B}_{n_s} \otimes \tilde{\mathbf{s}}_m^*(iN_s+n_s)] \tag{14}$$

where $\otimes$ denotes the Kronecker product. Clearly, without any blocking ($K = 1$), our ST block codes of (14) reduce to those in [2] and [15]. For example, when $N_t = 2$, we obtain from (11) that

$$\mathbf{A}_0 = \begin{bmatrix} 1 & 0 \\ 0 & 0 \end{bmatrix} \qquad \mathbf{A}_1 = \begin{bmatrix} 0 & 1 \\ 0 & 0 \end{bmatrix}$$
$$\mathbf{B}_0 = \begin{bmatrix} 0 & 0 \\ 0 & 1 \end{bmatrix} \qquad \mathbf{B}_1 = \begin{bmatrix} 0 & 0 \\ -1 & 0 \end{bmatrix} \tag{15}$$

and it follows from (14) that

$$\overline{\mathbf{S}}_m(i) = \begin{bmatrix} \overline{\mathbf{s}}_{m1}(2i) & \overline{\mathbf{s}}_{m2}(2i) \\ \overline{\mathbf{s}}_{m1}(2i+1) & \overline{\mathbf{s}}_{m2}(2i+1) \end{bmatrix} = \begin{bmatrix} \tilde{\mathbf{s}}_m(2i) & \tilde{\mathbf{s}}_m(2i+1) \\ -\tilde{\mathbf{s}}_m^*(2i+1) & \tilde{\mathbf{s}}_m^*(2i) \end{bmatrix} \tag{16}$$

which is nothing but the block counterpart of [2]. Our ST encoder design is summarized as follows:

d2.1) given N_t, select N_s, N_d according to (12);
d2.2) find $\mathcal{O}_{N_t}$ of size $N_d \times N_t$ with rate $R = N_s/N_d$;
d2.3) use (13) to obtain $\{\mathbf{A}_{n_s}, \mathbf{B}_{n_s}\}_{n_s=0}^{N_s-1}$;
d2.4) build the ST block codes $\overline{\mathbf{S}}_m(i)$ according to (14).

Given the MUI-free received blocks $\mathbf{y}_m(n)$ of (10), we will exploit next the available transmit diversity embedded in (2) to recover $\mathbf{s}_m(n)$ with diversity gain. The channel matrices $\{\mathcal{D}_{mn_t}\}_{n_t=1}^{N_t}$ are supposed available and will be assumed time-invariant for at least N_d blocks.

C. Block ST Decoder Design

Defining the $Q \times Q$ diagonal matrix $\mathcal{D}_{\overline{\mathbf{s}}_{mn_t}}(n) := \text{diag}[\overline{s}_{mn_t}(nQ), \ldots, \overline{s}_{mn_t}(nQ+Q-1)]$ and the $Q \times 1$ channel vector $\mathbf{h}_{mn_t} := [H_{mn_t}(\rho_{m,0}), \ldots, H_{mn_t}(\rho_{m,Q-1})]^T$, we use the identity $\mathcal{D}_{mn_t}\overline{\mathbf{s}}_{mn_t}(n) = \mathcal{D}_{\overline{\mathbf{s}}_{mn_t}}(n)\mathbf{h}_{mn_t}$ to rewrite (10) as

$$\mathbf{y}_m(n) = A_m \sum_{n_t=1}^{N_t} \mathcal{D}_{\overline{\mathbf{s}}_{mn_t}}(n)\mathbf{h}_{mn_t} + \boldsymbol{\eta}_m(n). \tag{17}$$

Let us collect N_d consecutive blocks $\mathbf{y}_m(n)$ into a superblock $\tilde{\mathbf{y}}_m(i) := [\mathbf{y}_m^T(iN_d), \ldots, \mathbf{y}_m^T(iN_d + N_d - 1)]^T$ and use (17) to obtain

$$\tilde{\mathbf{y}}_m(i) = A_m \underbrace{\begin{bmatrix} \boldsymbol{\mathcal{D}}_{\bar{s}_{m1}}(iN_d) & \cdots & \boldsymbol{\mathcal{D}}_{\bar{s}_{mN_t}}(iN_d) \\ \vdots & & \vdots \\ \boldsymbol{\mathcal{D}}_{\bar{s}_{m1}}(iN_d+N_d-1) & \cdots & \boldsymbol{\mathcal{D}}_{\bar{s}_{mN_t}}(iN_d+N_d-1) \end{bmatrix}}_{:=\mathbf{D}_{\bar{s}_m}(i)} \times \begin{bmatrix} \mathbf{h}_{m1} \\ \vdots \\ \mathbf{h}_{mN_t} \end{bmatrix} + \tilde{\boldsymbol{\eta}}_m(i) \tag{18}$$

where $\tilde{\boldsymbol{\eta}}_m(i)$ is defined similar to $\tilde{\mathbf{y}}_m(i)$. By comparing $\mathbf{D}_{\bar{s}_m}(i)$ [defined under (18)] to $\overline{\mathbf{S}}_m(i)$ of (2), we infer from (14) that

$$\mathbf{D}_{\bar{s}_m}(i) = \sum_{n_s=0}^{N_s-1} [\mathbf{A}_{n_s} \otimes \boldsymbol{\mathcal{D}}_{\tilde{s_m}}(iN_s+n_s) + \mathbf{B}_{n_s} \otimes \boldsymbol{\mathcal{D}}^*_{\tilde{s_m}}(iN_s+n_s)] \tag{19}$$

where $\boldsymbol{\mathcal{D}}_{\tilde{s_m}}(n) := \mathrm{diag}[\tilde{s}_m(nQ), \ldots, \tilde{s}_m(nQ+Q-1)]^T$. Plugging (19) into (18) and using the identity $\boldsymbol{\mathcal{D}}_{\tilde{s_m}}(n)\mathbf{h}_{mn_t} = \boldsymbol{\mathcal{D}}_{mn_t}\tilde{\mathbf{s}}_m(n)$, we obtain

$$\tilde{\mathbf{y}}_m(i) = A_m \sum_{n_s=0}^{N_s-1} \sum_{n_t=1}^{N_t} \times \{[\mathbf{A}_{n_s}(:, n_t) \otimes \boldsymbol{\mathcal{D}}_{mn_t}]\tilde{\mathbf{s}}_m(iN_s+n_s) + [\mathbf{B}_{n_s}(:, n_t) \otimes \boldsymbol{\mathcal{D}}_{mn_t}]\tilde{\mathbf{s}}^*_m(iN_s+n_s)\} + \tilde{\boldsymbol{\eta}}_m(i). \tag{20}$$

Our ST decoder $\overline{\mathcal{E}}(\cdot)$ consists of N_s branches of detectors each described by the $Q \times 2N_dQ$ partitioned matrix $\boldsymbol{\mathcal{L}}_{m,n_s}$ as follows:

$$\boldsymbol{\mathcal{L}}_{m,n_s} := \left[\sum_{n_t=1}^{N_t} \mathbf{A}^T_{n_s}(:, n_t) \otimes \boldsymbol{\mathcal{D}}^*_{mn_t} \middle| \sum_{n_t=1}^{N_t} \mathbf{B}^T_{n_s}(:, n_t) \otimes \boldsymbol{\mathcal{D}}_{mn_t} \right]. \tag{21}$$

To decode $\tilde{\mathbf{s}}_m(iN_s + n_s)$ with diversity gain, we concatenate $\tilde{\mathbf{y}}_m(i)$ and its conjugate and premultiply the result by $\boldsymbol{\mathcal{L}}_{m,n_s}$ to output the $Q \times 1$ block $\mathbf{z}_m(iN_s + n_s)$ as

$$\mathbf{z}_m(iN_s + n_s) = \boldsymbol{\mathcal{L}}_{m,n_s} \begin{bmatrix} \tilde{\mathbf{y}}_m(i) \\ \tilde{\mathbf{y}}^*_m(i) \end{bmatrix}. \tag{22}$$

Substituting (21) into (22), we prove in the Appendix that

$$\begin{aligned} \mathbf{z}_m(iN_s+n_s) &= \alpha A_m \left(\sum_{n_t=1}^{N_t} \boldsymbol{\mathcal{D}}^*_{mn_t}\boldsymbol{\mathcal{D}}_{mn_t} \right) \tilde{\mathbf{s}}_m(iN_s+n_s) + \check{\boldsymbol{\eta}}_m(iN_s+n_s) \\ &= \alpha A_m \boldsymbol{\mathcal{D}}_m \boldsymbol{\Theta}_m \mathbf{s}_m(iN_s+n_s) + \check{\boldsymbol{\eta}}_m(iN_s+n_s) \end{aligned} \tag{23}$$

where for the second equality we used (1) and the definitions $\boldsymbol{\mathcal{D}}_m := \sum_{n_t=1}^{N_t} \boldsymbol{\mathcal{D}}^*_{mn_t}\boldsymbol{\mathcal{D}}_{mn_t} = \mathrm{diag}[\sum_{n_t=1}^{N_t} |H_{mn_t}(\rho_{m,0})|^2, \ldots, \sum_{n_t=1}^{N_t} |H_{mn_t}(\rho_{m,Q-1})|^2]$ and $\check{\boldsymbol{\eta}}_m(iN_s + n_s) := \boldsymbol{\mathcal{L}}_{m,n_s}[\tilde{\boldsymbol{\eta}}^T_m(i)\tilde{\boldsymbol{\eta}}^{*T}_m(i)]^T$. Equation (23) shows how N_t-fold transmit diversity has been gained through $\boldsymbol{\mathcal{D}}_m$. For example, when $N_t = 2(N_s = N_d = 2)$, the two branches of our ST decoder $\overline{\mathcal{E}}(\cdot)$ are given by [cf. (15) and (21)]

$$\begin{bmatrix} \boldsymbol{\mathcal{L}}_{m,0} \\ \boldsymbol{\mathcal{L}}_{m,1} \end{bmatrix} = \begin{bmatrix} \boldsymbol{\mathcal{D}}^*_{m1} & \mathbf{0}_{Q\times Q} & \mathbf{0}_{Q\times Q} & \boldsymbol{\mathcal{D}}_{m2} \\ \boldsymbol{\mathcal{D}}^*_{m2} & \mathbf{0}_{Q\times Q} & \mathbf{0}_{Q\times Q} & -\boldsymbol{\mathcal{D}}_{m1} \end{bmatrix}. \tag{24}$$

Substituting (24) into (22), the two output blocks $\mathbf{z}_m(iN_s)$ and $\mathbf{z}_m(iN_s + 1)$ can be formed as

$$\begin{bmatrix} \mathbf{z}_m(2i) \\ \mathbf{z}_m(2i+1) \end{bmatrix} = \begin{bmatrix} \boldsymbol{\mathcal{D}}^*_{m1} & \boldsymbol{\mathcal{D}}_{m2} \\ \boldsymbol{\mathcal{D}}^*_{m2} & -\boldsymbol{\mathcal{D}}_{m1} \end{bmatrix} \begin{bmatrix} \mathbf{y}_m(2i) \\ \mathbf{y}^*_m(2i+1) \end{bmatrix}. \tag{25}$$

Having decoded our block ST transmissions, our next subsection will illuminate the importance of redundant precoding that we introduced in $\boldsymbol{\Theta}_m$.

D. Precoder Design for Guaranteed Symbol Recovery

Following the precoding ideas of [4] and [19], this subsection will rely on $\mathbf{z}_m(iN_s + n_s)$ to recover the information symbols $\mathbf{s}_m(iN_s + n_s)$. It is deduced from (23) that the necessary and sufficient condition to retrieve $\mathbf{s}_m(iN_s + n_s)$ with a linear equalizer *regardless* of the information symbol constellation is to have [4]

$$\mathrm{rank}(\boldsymbol{\mathcal{D}}_m\boldsymbol{\Theta}_m) \geq K. \tag{26}$$

Constellation-independent linear equalizers are desirable from a computational perspective and useful for initializing constant-modulus and decision-feedback (DF) alternatives. Furthermore, linear constellation-irrespective equalizers obviate error-propagation effects.

Since $h_{mn_t}(l)$ has order $\leq L$, at most L of $\{H_{mn_t}(\rho_{m,q})\}_{q=0}^{Q-1}$ can be zero. However, it is very unlikely to have $\sum_{n_t=1}^{N_t} |H_{mn_t}(\rho_{m,q})|^2 = 0$, when each user's channels are uncorrelated. If we ignore this chance, we just choose $Q = K$ and $\boldsymbol{\Theta}_m = \mathbf{I}$ in (1). But even when channels are correlated and $\boldsymbol{\mathcal{D}}_m$ loses rank due to common channel nulls, we can still guarantee symbol recovery using the redundant precoders of [4] and [19]. Recognizing that in the worst case, $\mathrm{rank}(\boldsymbol{\mathcal{D}}_m) = Q - L$, we design our redundant precoder $\boldsymbol{\Theta}_m$ to satisfy: $Q = K + L$ and any K rows of $\boldsymbol{\Theta}_m$ to be linearly independent. One simple choice of $\boldsymbol{\Theta}_m$ is

$$\boldsymbol{\Theta}_m = \begin{bmatrix} 1 & \rho^{-1}_{m,0} & \cdots & \rho^{-(K-1)}_{m,0} \\ 1 & \rho^{-1}_{m,1} & \cdots & \rho^{-(K-1)}_{m,1} \\ \vdots & \vdots & & \vdots \\ 1 & \rho^{-1}_{m,Q-1} & \cdots & \rho^{-(K-1)}_{m,Q-1} \end{bmatrix} \tag{27}$$

where the mth user's signature points $\{\rho_{m,q}\}_{q=0}^{Q-1}$ are distinct so that any K rows of the Vandermonde matrix in (27) are linearly independent. Redundancy and judicious choice of the precoder $\boldsymbol{\Theta}_m$ [as in (27)] satisfies condition (26) for any channel matrix $\boldsymbol{\mathcal{D}}_m$ which assures symbol recovery no matter what FIR channel

is encountered. In a way, redundant precoding "shapes the ISI channels" to ensure an invertible one-to-one input–output relationship. Furthermore, $\mathbf{\Theta}_m$ introduces extra diversity (over the complex field) in addition to the ST diversity gained through the GCOD.

Depending on complexity versus performance tradeoffs, *any single user linear equalizer* can be applied to retrieve $\mathbf{s}_m(n)$ from (23). For example, we may choose the zero-forcing (ZF) equalizer (see also Fig. 1) which is given by

$$\mathbf{\Gamma}_m = (\mathcal{D}_m \mathbf{\Theta}_m)^{\dagger}. \tag{28}$$

Now we summarize our overall design as follows.

Theorem 1: Assuming that the channels are FIR and time-invariant at least over N_d received blocks, the design steps d1.1)–d1.3) and d2.1)–d2.4) guarantee deterministic MUI elimination, symbol recovery, and transmit diversity gain of our system in Fig. 1, regardless of each user's frequency-selective channels.

Some remarks are due at this point.

Remark 1: The proposed system of Fig. 1 is applicable to both the uplink and the downlink. However, since only one antenna is required at the receiver, our proposed system is especially attractive for downlink applications. For the downlink, transmissions for all M users originate at the base station and they share the same multiple transmit antennas. In this case, a total of N_t instead of MN_t antennas are deployed at the base station. With $M = 1$ and skipping the MUI elimination stage, our multiple-access design is also applicable to the single-user setting that is dealt with in [5], [6], [8], and [21]. It is in fact that only ST block-coded single-user system that guarantees symbol recovery regardless of frequency-selective propagation.

Remark 2: One advantage of our design (inherited from [4] and [19]) is that MUI is eliminated without requiring CSI at the receiver. Thus, the number of channels to be estimated for each user's symbol recovery is N_t instead of MN_t. Blind estimation of multiple channels with a single receive antenna is challenging. For a single user with two transmit antennas, blind channel estimation has been reported in [8] and [21] relying on a deterministic constant modulus algorithm, and in [9] using a subspace method with time-varying (TV) redundant precoding. Without TV precoding, constellation irrespective blind channel estimation in our multiuser scenario is also possible using an "antenna switching" method, where for estimating $h_{m\overline{n}_t}(l)$ only the $\overline{n}_t$th antenna is switched on, while all $n_t \neq \overline{n}_t$ antennas are off. Because only a single channel has to be estimated at the receiver, any single channel estimator is applicable. However, by using "antenna switching" for channel estimation, the system becomes "uncoded" when acquiring CSI and no diversity gain is achieved. The simulations of Section VI will indicate that our system outperforms OFDM even with uncoded transmissions through multipath channels. To maintain an overall blind and simple receiver, it is also possible to use the blind channel estimator based on the filterbank approach of [13]. Such a blind channel estimator capitalizes on input redundancy which is also present in our transmitter design in the form of L guard zeros. The simulations of Section VI will illustrate its reliable performance.

Remark 3: We infer from (23) that the normalized equivalent channel gain for $\tilde{s}_m(nQ+q)$ is $G_m(q) := (1/N_t)\sum_{n_t=1}^{N_t} |H_{mn_t}(\rho_{m,q})|^2$. Since $G_m(q)$ is the sum of squares of $H_{mn_t}(\rho_{m,q})$, the equivalent channel in our system can be zero or weak only if $H_{mn_t}(\rho_{m,q})$s for all n_t are zero or weak. In [11], however, the equivalent channel gain after MUI suppression is the sum of squares of linear (beamformed) combinations of multiple-antenna channels. Hence, the equivalent channel could be zero or weak even when the multiantenna channels themselves are strong. Thus, the performance of each user may suffer considerably from the beamforming-based MUI suppression of [11], which is not the case for our system, as we will discuss in the next section. Observe that $G_m(q)$ depends also on the choice of signature points. If CSI is available at the transmitter, e.g., via a feedback channel, we have flexibility to optimize the allocation of signature points $\rho_{m,q}$. If the channels are unknown to the transmitter, then similar to [20] and [23], hopping the signature points may be helpful to avoid persistent fading. These issues are interesting future directions, but their thorough analysis goes beyond the scope of this paper.

V. Design Considerations

So far we have designed a general ST coded multiuser transceiver that guarantees symbol recovery with transmit diversity gain regardless of the underlying frequency-selective channels. In this section, we further consider the choice of design parameters taking into account practical issues such as complexity, efficiency, and performance.

A. Overall Bandwidth Efficiency

Redundancy has been exploited so far in three places, correspondingly for three purposes: i) IBI elimination (through L guard zeros); ii) guaranteed symbol recovery (through redundant precoding); and iii) ST coding for $N_t > 2$ transmit antennas. Because redundancy certainly affects the information rate, it is of interest to check the bandwidth efficiency of our designs.

As described in Sections III and IV, the transmitted block has length $J = P+L = M(K+L)+L$ including the L guard zeros ($P = MQ$ and $Q = K+L$). From the viewpoint of bandwidth utilization, each of the M users sends N_s information blocks of length K for every N_d transmitted blocks of length J (see also Section II). Therefore, the overall bandwidth efficiency of our ST coded multiuser system is

$$\xi = \frac{MN_sK}{N_d[M(K+L)+L]} = \begin{cases} \dfrac{MK}{M(K+L)+L}, & \text{if } N_t = 2 \\ \dfrac{3MK}{4M(K+L)+4L}, & \text{if } N_t = 3,\, 4 \\ \dfrac{MK}{2M(K+L)+2L}, & \text{if } N_t > 4 \end{cases} \tag{29}$$

where in deriving the second equality we used (12). Clearly, the overall bandwidth efficiency ξ depends on the ratio K/L. Re-

call that we consider in this paper a QS multiuser system (see Section II) where quasi-synchronism among all users ensures that the channel order L is relatively small. Hence, for a sufficiently (but reasonably) large $K \gg L$, we will have $\xi \simeq 1$ when $N_t = 2$; however, $\xi \simeq 0.75$ when $N_t = 3, 4$ and $\xi \simeq 0.5$ when $N_t > 4$. Hence, similar to [15], the bandwidth efficiency is sacrificed only when $N_t > 2$ transmit antennas are deployed. On the other hand, (23) implies that higher diversity gains can be achieved with more than two transmit antennas. By regaining bandwidth efficiency through larger constellation sizes, we will see in Section VI that the overall performance improves as the number of transmit antennas increases.

B. Signature Point Selection and Allocation

Step d1.2) does not specify how to select the signature points ρ_p and decide their allocation $\mathcal{I}_\mu$. The optimal design of ρ_p and $\mathcal{I}_\mu$ may rely on CSI knowledge at the transmitter (see also Remark 3 of Section IV) which may not be practical for wireless access and will not be pursued in this paper. However, we consider herein a particular choice of ρ_ps which leads to low-complexity designs. Specifically, similar to [4] and [19], we recommend selecting ρ_ps regularly spaced around unit circle on the FFT grid, i.e., we choose as signature points

$$\rho_p = e^{j(2\pi/P)p} \qquad \forall\, p \in [0,\, P-1]. \tag{30}$$

Plugging (30) into (7) leads to $\boldsymbol{\mathcal{V}}_1 = \mathbf{F}$ and $\boldsymbol{\mathcal{V}}_2 = \mathbf{F}\mathbf{R}_{\text{oa}}$, where $\mathbf{F}$ is the $P \times P$ FFT matrix and $\mathbf{R}_{\text{oa}} := [\mathbf{I}_P \mathbf{I}_{\text{oa}}]$ is a $P \times (P+L)$ matrix implementing the overlap-add (oa) operation.[3] Accordingly, the user spreading code $\mathbf{C}_\mu$ and the user separating filter $\mathbf{G}_\mu$ become $\mathbf{C}_\mu = \mathbf{F}^{\mathcal{H}}\boldsymbol{\Phi}_\mu$ and $\mathbf{G}_\mu = \boldsymbol{\Phi}_\mu^T \mathbf{F}\mathbf{R}_{\text{oa}}$, which suggests that the matrix multiplication by $\mathbf{C}_\mu$ and $\mathbf{G}_\mu$ can be implemented by low-complexity FFTs. Note also that the entries of the matrices $\boldsymbol{\Phi}_\mu$ and $\mathbf{R}_{\text{oa}}$ are either 0 or 1 and thus their operation involves simple addition. As a result, our design has low complexity if the choice of ρ_ps in (30) is adopted.

Selecting ρ_js to be complex exponentials as in (30) corresponds to an OFDM-like multiuser system with a total of P subcarriers allocated to M users. The subcarrier allocation is specified through the choice of the index subsets $\mathcal{I}_\mu$ in (6). Two possible choices for $\mathcal{I}_\mu$'s are, $\forall \mu \in [0,\, M-1]$

$$\mathcal{I}_\mu = \{\nu M + \mu + 1,\, \nu = 0, \ldots, Q-1\} \tag{31a}$$

$$\mathcal{I}_\mu = \{\mu Q + \nu + 1,\, \nu = 0, \ldots, Q-1\}. \tag{31b}$$

The choice (31a) assigns P subcarriers periodically interleaved to M users as in the generalized OFDMA (G-OFDMA) system of [4] and [19], while (31b) corresponds to a digital FDMA assignment where each user is allocated Q contiguous subcarriers. Because Q signature points designate Q subchannels [see the definition of $\boldsymbol{\mathcal{D}}_m$ in (23)] for every user, the allocation of (31a) renders these subchannels more uncorrelated than the subchannels corresponding to (31b), and thus increases diversity. Consequently, the chance that the subchannels corresponding to (31a) suffer from deep fades simultaneously is lower than that corresponding to (31b). The comparison between (31a) and (31b) will be investigated also through simulations in Section VI.

[3]Indeed, with $\mathbf{I}_{\text{oa}}$ denoting the first L columns of the $P \times P$ identity matrix $\mathbf{I}_P$, it is shown in [19] that when $\mathbf{R}_{\text{oa}}$ multiplies a $(P+L) \times 1$ vector $\mathbf{v}$, it yields a $P \times 1$ vector $\mathbf{v}_{\text{oa}} := \mathbf{R}_{\text{oa}}\mathbf{v}$ whose top L entries are superpositions of the bottom L with the top L entries of $\mathbf{v}$ (see also [10] and [22] for details).

C. Performance Versus Complexity Tradeoffs

The MUI-elimination design in Section III converts an M-user system into M single-user systems and greatly reduces not only the receiver complexity but also the burden of multichannel estimation, as well as timing acquisition and synchronization. However, the price paid is a slight performance loss by coloring the noise $\boldsymbol{\eta}_m(n)$ in (10). Let us consider the special choice of ρ_p in (30). It follows from the definition of $\boldsymbol{\eta}_m(n)$ that its correlation matrix can be written as

$$\boldsymbol{\Lambda}_{\eta_m} = N_0 \boldsymbol{\Phi}_m^T \boldsymbol{\mathcal{V}}_2 \boldsymbol{\mathcal{V}}_2^H \boldsymbol{\Phi}_m = N_0 \boldsymbol{\Phi}_m^T (P\mathbf{I}_P + \mathbf{F}\mathbf{I}_{\text{oa}}\mathbf{I}_{\text{oa}}^{\mathcal{H}}\mathbf{F}^H)\boldsymbol{\Phi}_m \tag{32}$$

where N_0 is the power spectral density of $w(n)$. It is easy to verify that the maximum entry of the matrix $\mathbf{F}\mathbf{I}_{\text{oa}}\mathbf{I}_{\text{oa}}^{\mathcal{H}}\mathbf{F}^{\mathcal{H}}$ is L. If we choose $K \gg L$ (and thus $P \gg L$), the matrix $\boldsymbol{\Lambda}_{\eta_m}$ can be well approximated as: $\boldsymbol{\Lambda}_{\eta_m} \approx N_0 P \mathbf{I}_Q$. For sufficiently large K, the residual noise $\boldsymbol{\eta}_m(n)$ will thus be approximately white in which case the loss introduced by MUI elimination will be negligible. Note also that with $\boldsymbol{\eta}_m(n)$ being white, the noise terms $\check{\boldsymbol{\eta}}_m(iN_s + n_s)$ in (23) for different n_s become uncorrelated. Hence, separating the detection of $\tilde{\mathbf{s}}_m(iN_s + n_s)$ from that of $\tilde{\mathbf{s}}_m(iN_s + n_s')$, $\forall\, n_s' \neq n_s$ will not incur any performance loss. Thus, as far as performance and bandwidth efficiency are concerned, choosing a large K is preferable. But as K increases, the detection delay increases as well, since the receiver has to wait for $N_d[M(K+L)+L]$ received symbols to perform ST decoding. Furthermore, as K increases, the receiver complexity grows accordingly. Recall that our ST decoding in Section IV requires that channels remain invariant for at least N_d blocks of length $J = M(K+L)+L$. Thus, increasing K also requires longer channel coherence time. In practice, how large K should be depends on complexity versus performance tradeoffs and the application environment.

VI. Performance Analysis and Comparison

Assuming $w(n)$ in (3) is AWGN with spectral density N_0, theoretical BER evaluation is possible for a given constellation when we adopt the ZF equalizer of (28). Starting with (23), the decision vector $\hat{\mathbf{s}}_m(iN_s + n_s) := \boldsymbol{\Gamma}_m \mathbf{z}_m(iN_s + n_s)$ for $\mathbf{s}_m(iN_s + n_s)$ is given by

$$\check{\mathbf{z}}_m(iN_s + n_s) = \alpha A_m \mathbf{s}_m(iN_s + n_s) + \overline{\boldsymbol{\eta}}_m(iN_s + n_s) \tag{33}$$

where $\overline{\boldsymbol{\eta}}_m(iN_s + n_s) := (\boldsymbol{\mathcal{D}}_m \boldsymbol{\Theta}_m)^\dagger \check{\boldsymbol{\eta}}_m(iN_s + n_s)$. We deduce from the definition of $\check{\boldsymbol{\eta}}_m(iN_s + n_s)$ and straightforward matrix manipulations that

$$\check{\boldsymbol{\eta}}_m(iN_s + n_s) = \boldsymbol{\mathcal{L}}_{m,\, n_s} \tilde{\mathbf{G}}_m \tilde{\mathbf{w}}(i) \tag{34}$$

where the $2N_dQ \times 2N_dJ$ matrix $\tilde{\mathbf{G}}_m$ and the $2N_dJ \times 1$ vector $\tilde{\mathbf{w}}(i)$ are given by

$$\tilde{\mathbf{G}}_m := \begin{bmatrix} \mathbf{I}_{N_d} \otimes \mathbf{G}_m & \mathbf{0}_{N_dQ \times N_dJ} \\ \mathbf{0}_{N_dQ \times N_dJ} & \mathbf{I}_{N_d} \otimes \mathbf{G}_m^* \end{bmatrix}$$

$$\tilde{\mathbf{w}}(i) := \begin{bmatrix} \mathbf{w}(iN_d) \\ \vdots \\ \mathbf{w}(iN_d + N_d - 1) \\ \mathbf{w}^*(iN_d) \\ \vdots \\ \mathbf{w}^*(iN_d + N_d - 1) \end{bmatrix}. \tag{35}$$

Let us define the $K \times 2N_dJ$ matrix $\mathbf{\Phi}_m(n_s) := (\mathcal{D}_m\mathbf{\Theta}_m)^\dagger \mathcal{L}_{m,n_s}\tilde{\mathbf{G}}_m$, whose kth row is denoted by $\boldsymbol{\phi}_{m,k}^T(n_s)$, and write out (33) componentwise, $\forall k \in [0,\ K-1]$

$$\hat{s}_m((iN_s + n_s)K + k) = \alpha A_m s_m((iN_s + n_s)K + k) + \boldsymbol{\phi}_{m,k}^{\mathcal{H}}(n_s)\tilde{\mathbf{w}}_m(i). \tag{36}$$

To proceed further with our performance analysis, we assume quadrature phase-shift keying (QPSK) modulated transmissions. Our figure of merit is the average BER, defined as $\overline{P}_e = (N_sK)^{-1}\sum_{n_s=0}^{N_s-1}\sum_{k=0}^{K-1} P_{n_s,k}$, where $P_{n_s,k}$ denotes the BER for $s_m((iN_s + n_s)K + k)$ whose symbol energy we denote by E_s. It follows from (36) that

$$\overline{P}_e = (N_sK)^{-1}\sum_{n_s=0}^{N_s-1}\sum_{k=0}^{K-1} \mathcal{Q}\left(\sqrt{\frac{\alpha^2 A_m^2 E_s}{N_0 \boldsymbol{\phi}_{m,k}^{\mathcal{H}}(n_s)\boldsymbol{\phi}_{m,k}(n_s)}}\right). \tag{37}$$

Apart from the closed-form BER expression in (37), we will test the performance and reveal additional features of our system with simulated examples.

In all simulations, signature points are chosen as in (30) and their allocation is described by (31a) unless specified otherwise. Channels are assumed to be zero-mean Rayleigh faded with unit variance. The simulated BER is averaged over 200 channel and noise realizations for each E_b/N_0 point.

Example 1 (Single-User Performance and Comparison with OFDM): We test our system on a single-user ($M = 1$) setup with $N_t = 1, 2, 3, 4$ antennas and compare it with a single-antenna OFDM. The channels are assumed flat ($L = 0$). For $N_t = 1$ (uncoded) and $N_t = 2$ transmit antennas, 8-PSK modulation is used. But for fairness, 16-QAM modulation is adopted for $N_t = 3, 4$ transmit antennas so that bandwidth efficiency for different number of transmit antennas is identical. In OFDM, 32 subcarriers are used and 8-PSK modulation is employed. We choose block length parameters as: $Q = K = 32$. From Fig. 2, it is seen that our uncoded ($N_t = 1$) system's performance coincides with that of OFDM over the flat fading channel. However, with multiple transmit antennas our system outperforms OFDM. For example, our system with $N_t = 2, 3, 4$ transmit antennas gives, respectively, about one, two, and three orders of magnitude better performance than OFDM at an SNR of 20 dB. For

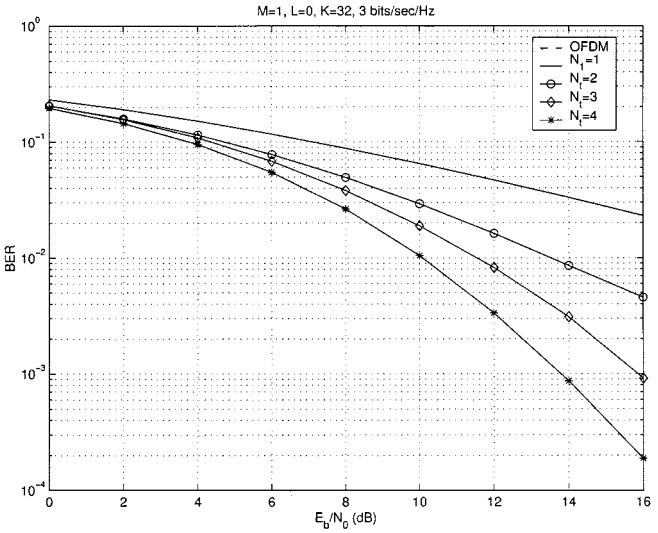

Fig. 2. Single user with flat fading channels.

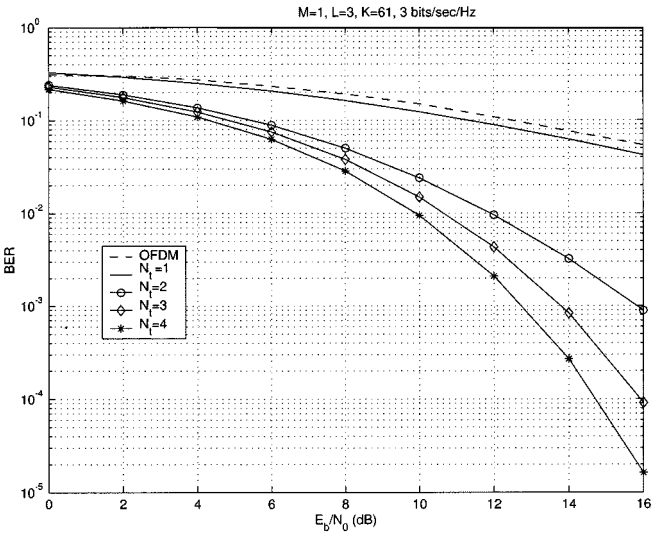

Fig. 3. Single user with frequency-selective channels.

frequency-selective channels of order $L = 3$ and block length parameters: $Q = 64$ and $K = 61$, the simulation is performed and the results are depicted in Fig. 3. Interestingly, even without ST coding, our uncoded ($N_t = 1$) system still outperforms OFDM. To explain the improvement, note that even without ST coding, each user in our system transmits over $K + L$ subcarriers instead of K used in OFDM. Consequently, our system does not suffer from deep channel fades (nulls) as discussed in Section III. With multiple transmit antennas, our system outperforms OFDM and the uncoded system significantly.

Example 2 (Multiuser Performance): We implement our system with multiple ($M = 16$) users with different N_ts and block length parameters $Q = 64$ and $K = 61$. Again, 8-PSK modulation is employed for $N_t = 1, 2$ and 16-QAM for $N_t = 3, 4$. Channels are assumed to be frequency-selective of order $L = 3$. Fig. 4 confirms that ST coding with multiple transmit antennas improves performance considerably in multiuser environments.

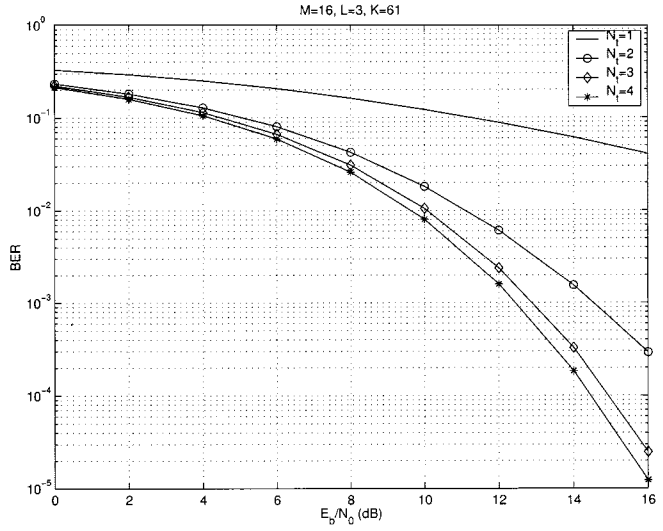

Fig. 4. Sixteen users with frequency-selective channels.

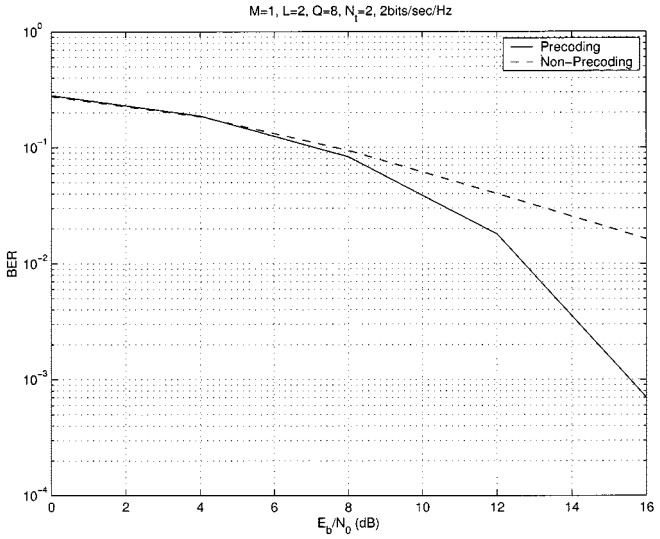

Fig. 6. Precoding for a specific frequency-selective channel.

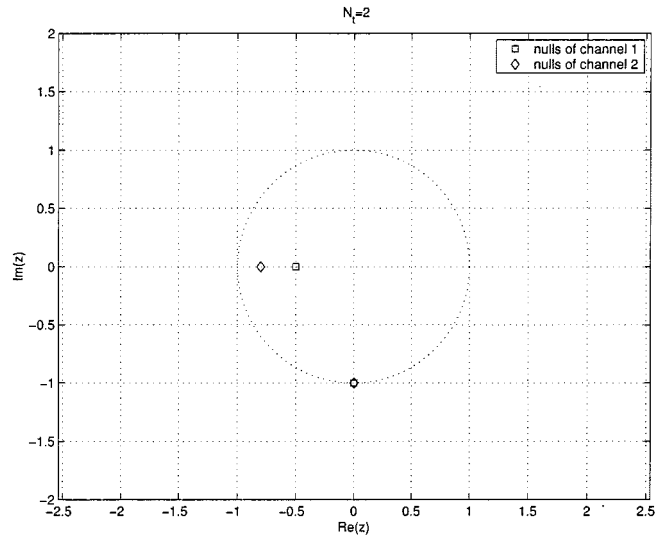

Fig. 5. Channel nulls.

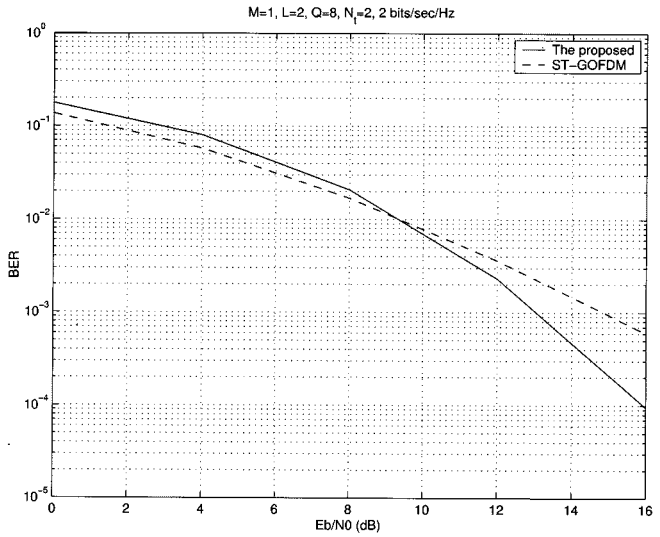

Fig. 7. Comparison with ST GOFDM [8], [21].

Example 3 (The Role of Redundant Precoding): Suppose $L = 2$, $M = 1$, $Q = 8$, $N_t = 2$, and QPSK modulation is employed. Two discrete-time equivalent channels are chosen to be $H_{m1}(z) = (1 + jz^{-1})(1 + 0.5z^{-1})$ and $H_{m2}(z) = (1 + jz^{-1})(1 + 0.8z^{-1})$. As shown in Fig. 5, two channels share a common zero at $\rho_6 = -j$. The BERs with redundant precoder $\mathbf{\Theta}_m$ and without $\mathbf{\Theta}_m$ are shown in Fig. 6. It is seen that the system with $\mathbf{\Theta}_m$ improves performance considerably at least for this particular pair of channels. With $\mathbf{\Theta}_m$ as in (27) and under the same system setup, we average BER over 200 independent channel realizations and compare our system to ST coded GOFDM in [8] and [21] where eight subcarriers are used. The results in Fig. 7 confirm that our system with $\mathbf{\Theta}_m$ outperforms [8] and [21]. It is important to remark that channel fading may be slow and different channels may share common nulls for a long time in some scenarios. Hence, we recommend using the precoder $\mathbf{\Theta}_m$ in our system.

Example 4 (Importance of Signature Point Allocation): Our system designs in Sections III and IV provide flexibility to allocate signature points to different users through the design of $\mathcal{I}_\mu$. To investigate the effects of signature allocation on BER performance, we compare the two allocation schemes specified in (31a) (G-OFDMA) and (31b) (FDMA), respectively. We choose parameters $M = 8$, $K = 61$, $L = 3$, $N_t = 2$, and QPSK modulation. The result depicted in Fig. 8 illustrates that the allocation scheme of (31a) is better than that of (31b), especially at high SNR values. Although symbol recovery in our system does not depend on the allocation of signature points, this example implies that judicious signature point allocation is still possible even without CSI at the transmitter.

Example 5 (Estimation of Unknown Channels): To simulate performance of the antenna switching channel estimation approach alluded in Remark 2, we choose $N_t = 2$, $L = 1$, $M = 4$, $Q = 16$, and $K = 15$. During CSI acquisition, only one antenna is switched on each time so that multichannel estimation reduces to single-channel estimation at the receiver. For the single-user channel estimation, the blind approach of [13] is implemented with 32 received blocks used for single-channel

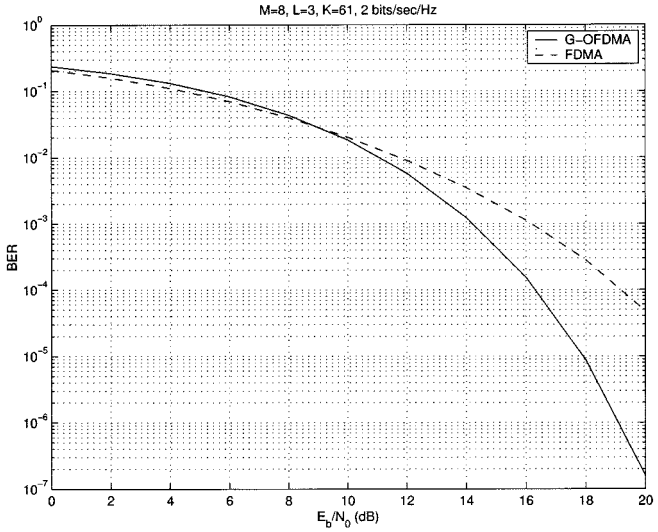

Fig. 8. Comparison with different signature allocation.

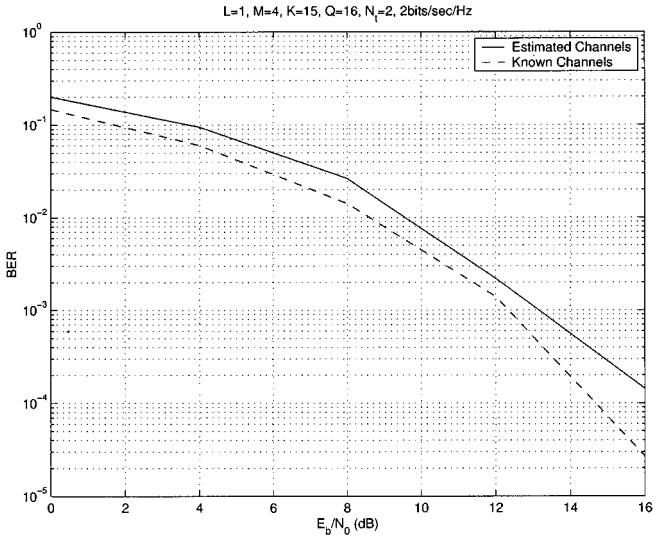

Fig. 9. BER with (un)known channels.

estimation (64 blocks for two channels). Once CSI has been acquired, our system reverts to its normal mode described in this paper. BER performance with estimated channels is shown against that with perfect CSI. The average BER is depicted in Fig. 9 where we observe that the blind method entails only a small penalty in the overall system performance.

VII. Conclusions and Discussion

We designed a novel ST coded multiuser system suitable for frequency-selective multipath fading channels. Relying on symbol blocking and ST redundancy, MUI was eliminated first, and novel ST block codes were designed next to achieve diversity gain. The system was shown capable of providing transmit diversity and guaranteed symbol recovery in multiuser environments regardless of the underlying FIR multipath. In addition to simplicity, simulations demonstrated the system's flexibility and superior performance.

This paper's ST coded multiuser system supports single-rate services and relies on a single receive antenna. The extensions to multirate services and multiple receive antennas are currently under investigation (see [14] for preliminary results). Another ongoing research topic is ST coding for doubly selective channels and adoption of the low-complexity finite alphabet based (semi) blind channel estimator of [20] and [23] to a G-OFDMA setting.

Appendix
Proof of (23)

Proof: According to the defining property of GCOD, namely, $\boldsymbol{\mathcal{O}}_{N_t}^{\mathcal{H}}\boldsymbol{\mathcal{O}}_{N_t} = \alpha(\sum_{n_s=0}^{N_s-1}|s_{n_s}|^2)\mathbf{I}$, we first deduce from (13) that

$$\mathbf{A}_{n_s}^T\mathbf{A}_{n_s'} + \mathbf{B}_{n_s}^T\mathbf{B}_{n_s'} = \begin{cases} \alpha\mathbf{I}_{N_t}, & \text{if } n_s = n_s' \\ \mathbf{0}_{N_t\times N_t}, & \text{if } n_s \neq n_s' \end{cases},$$
$$\mathbf{A}_{n_s}^T\mathbf{B}_{n_s'} = \mathbf{0}_{N_t\times N_t} \qquad \forall\, n_s,\, n_s'. \tag{38}$$

Neglecting the noise term $\tilde{\boldsymbol{\eta}}_m(i)$ from (20) and plugging (21) and (20) into (22), we obtain

$$\begin{aligned}
&\mathbf{z}_m(iN_s+n_s) \\
&\quad = A_m \sum_{n_s'=0}^{N_s-1}\sum_{n_t=1}^{N_t}\sum_{n_t'=1}^{N_t} \\
&\qquad \times \Big\{[\mathbf{A}_{n_s}^T(:,n_t')\otimes\boldsymbol{\mathcal{D}}_{mn_t'}^*][\mathbf{A}_{n_s'}(:,n_t)\otimes\boldsymbol{\mathcal{D}}_{mn_t}] \\
&\qquad\quad \times \tilde{\mathbf{s}}_m(iN_s+n_s') + [\mathbf{A}_{n_s}^T(:,n_t')\otimes\boldsymbol{\mathcal{D}}_{mn_t'}^*] \\
&\qquad\quad \times [\mathbf{B}_{n_s'}(:,n_t)\otimes\boldsymbol{\mathcal{D}}_{mn_t}]\tilde{\mathbf{s}}_m^*(iN_s+n_s') \\
&\qquad\quad + [\mathbf{B}_{n_s}^T(:,n_t')\otimes\boldsymbol{\mathcal{D}}_{mn_t'}][\mathbf{A}_{n_s'}(:,n_t)\otimes\boldsymbol{\mathcal{D}}_{mn_t}^*] \\
&\qquad\quad \times \tilde{\mathbf{s}}_m^*(iN_s+n_s') + [\mathbf{B}_{n_s}^T(:,n_t')\otimes\boldsymbol{\mathcal{D}}_{mn_t'}] \\
&\qquad\quad \times [\mathbf{B}_{n_s'}(:,n_t)\otimes\boldsymbol{\mathcal{D}}_{mn_t}^*]\tilde{\mathbf{s}}_m(iN_s+n_s')\Big\}.
\end{aligned} \tag{39}$$

Let us now recall the distributive property of Kronecker products of matrices (with appropriate dimensions): $(\mathbf{F}_1\otimes\mathbf{F}_2)(\mathbf{F}_3\otimes\mathbf{F}_4) = (\mathbf{F}_1\mathbf{F}_3)\otimes(\mathbf{F}_2\mathbf{F}_4)$. Applying this identity to (39) and exploiting (38), it follows readily that

$$\mathbf{z}_m(iN_s+n_s) = \alpha A_m \sum_{n_t=1}^{N_t}\boldsymbol{\mathcal{D}}_{mn_t}^*\boldsymbol{\mathcal{D}}_{mn_t}\tilde{\mathbf{s}}_m(iN_s+n_s) \tag{40}$$

which completes the proof of (23). ■

References

[1] D. Agrawal, V. Tarokh, A. Naguib, and N. Seshadri, "Space-time coded OFDM for high data-rate wireless communication over wideband channels," in *Proc. Vehicular Technology Conf.*, Ottawa, ON, Canada, May 18–21, 1998, pp. 2232–2236.

[2] S. M. Alamouti, "A simple transmit diversity technique for wireless communications," *IEEE J. Select. Areas Commun.*, vol. 16, pp. 1451–1458, Oct. 1998.

[3] V. M. DaSilva and E. S. Sousa, "Multicarrier orthogonal CDMA signals for quasisynchronous communication systems," *IEEE J. Select. Areas Commun.*, pp. 842–852, June 1994.

[4] G. B. Giannakis, Z. Wang, A. Scaglione, and S. Barbarossa, "AMOUR—Generalized multicarrier transceivers for blind CDMA regardless of multipath," *IEEE Trans. Commun.*, vol. 48, pp. 2064–2076, Dec. 2000.
[5] Y. Li, J. C. Chung, and N. R. Sollenberger, "Transmitter diversity for OFDM systems and its impact on high-rate data wireless networks," *IEEE J. Select. Areas Commun.*, vol. 17, pp. 1233–1243, July 1999.
[6] Y. Li, N. Seshadri, and S. Ariyavisitakul, "Channel estimation for OFDM systems with transmitter diversity in mobile wireless channels," *IEEE J. Select. Areas Commun.*, vol. 17, pp. 461–471, Mar. 1999.
[7] Z. Liu and G. B. Giannakis, "Space-time coding with transmit antennas for multiple access regardless of frequency-selective multipath," in *Proc. First Sensor Array and Multichannel Signal Processing Workshop*, Boston, MA, Mar. 15–17, 2000, pp. 178–182.
[8] Z. Liu, G. B. Giannakis, S. Barbarossa, and A. Scaglione, "Transmit-antennae space-time block coding for generalized OFDM in the presence of unknown multipath," IEEE J. Select. Areas Commun., to be published.
[9] Z. Liu, G. B. Giannakis, B. Muquet, and S. Zhou, "Space-time coding for broadband wireless communications," *Wireless Syst. Mobile Comput.*, vol. 1, no. 1, pp. 33–53, Jan.–Mar. 2001.
[10] B. Muquet, Z. Wang, G. B. Giannakis, M. de Courville, and P. Duhamel, "Cyclic prefix or zero-padding for multi-carrier transmissions?," IEEE Trans. Commun., submitted for publication.
[11] A. F. Naguib, N. Seshadri, and A. R. Calderbank, "Applications of space-time codes and interference suppression for high capacity and high data rate wireless systems," in *Proc. 32nd Annu. Asilomar Conf. Signals, Systems and Computers*, Pacific Grove, CA, Nov. 1998, pp. 1803–1810.
[12] A. F. Naguib, N. Seshadri, and R. Calderbank, "Space-time coding and signal processing for high data rate wireless communications," *IEEE Signal Processing Mag.*, vol. 17, pp. 76–92, May 2000.
[13] A. Scaglione, G. B. Giannakis, and S. Barbarossa, "Redundant filterbank precoders and equalizers—Part II: Blind channel estimation, synchronization, and direct estimation," *IEEE Trans. Signal Processing*, vol. 47, pp. 2007–2022, July 1999.
[14] A. Stamoulis, Z. Liu, and G. B. Giannakis, "Space-time coded generalized multicarrier CDMA with block-spreading for multirate services," in *Proc. 38th Allerton Conf.*, Monticello, IL, Oct. 4–6, 2000.
[15] V. Tarokh, H. Jafarkhani, and A. R. Calderbank, "Space-time block codes from orthogonal designs," *IEEE Trans. Inform. Theory*, vol. 45, pp. 1456–1467, July 1999.
[16] ——, "Space-time block coding for wireless communications: Performance results," *IEEE J. Select. Areas Commun.*, vol. 17, pp. 451–460, Mar. 1999.
[17] V. Tarokh, A. Naguib, N. Seshadri, and A. R. Calderbank, "Combined array processing and space-time coding," *IEEE Trans. Inform. Theory*, vol. 45, pp. 1121–1128, May 1999.
[18] V. Tarokh, N. Seshadri, and A. R. Calderbank, "Space-time codes for high data rate wireless communication: Performance criterion and code construction," *IEEE Trans. Inform. Theory*, vol. 44, pp. 744–765, Mar. 1998.
[19] Z. Wang and G. B. Giannakis, "Wireless multicarrier communications: Where Fourier meets Shannon," *IEEE Signal Processing Mag.*, vol. 17, pp. 29–48, May 2000.
[20] S. Zhou, G. B. Giannakis, and A. Scaglione, "Long codes for generalized FH-OFDMA through unknown multipath channels," *IEEE Trans. Commun.*, vol. 49, pp. 721–733, Apr. 2001.
[21] Z. Liu, G. B. Giannakis, S. Barbarossa, and A. Scaglione, "Transmit-antennae space-time block coding for generalized OFDM in the presence of unknown multipath," in *Proc. 33rd Asilomar Conf. Signals, Systems, and Computers*, Pacific Grove, CA, Nov. 1–4, 1999, pp. 1557–1561.
[22] B. Muquet, Z. Wang, G. B. Giannakis, M. de Courville, and P. Duhamel, "Cyclic prefix or zero-padding for multi-carrier transmissions?," in *Proc. Int. Conf. Communications*, New Orleans, LA, June 18–22, 2000, pp. 1049–1053.
[23] S. Zhou, G. B. Giannakis, and A. Scaglione, "Long codes for generalized FH-OFDMA through unknown multipath channels," in *Proc. Wireless Communications and Networking Conf.*, Chicago, IL, Sept. 23–28, 2000.
[24] S. Zhou and G. B. Giannakis, "Space–time coded transmissions with maximum diversity gains over frequency-selective multipath fading channels," IEEE Trans. Inform. Theory, submitted for publication.

Zhiqiang Liu received the B.S. degree from the Department of Radio and Electronics, Peking University, Beijing, China, in 1991, and the M.E. degree from the Institute of Electronics, Chinese Academy of Science, Beijing, China, in 1994. He received the Ph.D. degree from the Department of Electrical and Computer Engineering, University of Minnesota, Minneapolis, in 2001.

From 1995 to 1997, he was a Research Scholar at the Department of Electrical Engineering, National University of Singapore. From 1997 to 1998, he was a Research Assistant with the University of Virginia, Charlottesville. His research interests lie in the areas of wireless communications and signal processing, including space–time coding, wide-band wireless communication systems, multiuser detection, multicarrier, and blind channel estimation algorithms.

Georgios B. Giannakis (F'97) received the Diploma in electrical engineering from the National Technical University of Athens, Athens, Greece, in 1981. From September 1982 to July 1986, he was with the University of Southern California (USC), Los Angeles, where he received the MSc. degree in electrical engineering in 1983, the MSc. degree in mathematics in 1986, and the Ph.D. degree in electrical engineering in 1986.

After lecturing for one year at USC, he joined the University of Virginia, Charlottesville, in 1987, where he became a Professor of Electrical Engineering in 1997. Since 1999, he has been with the University of Minnesota, Minneapolis, as a Professor of Electrical and Computer Engineering. His general interests span the areas of communications and signal processing, estimation and detection theory, time-series analysis, and system identification—subjects on which he has published more than 120 journal papers, 250 conference papers, and two edited books. Current research topics focus on transmitter and receiver diversity techniques for single- and multiuser fading communication channels, redundant precoding and space–time coding for block transmissions, multicarrier, and wide-band wireless communication systems.

Dr. Giannakis has co-authored three papers that received Best Paper Awards from the IEEE Signal Processing (SP) Society (1992, 1998, 2000). He also received the Society's Technical Achievement Award in 2000. He co-organized three IEEE-SP Workshops (HOS in 1993, SSAP in 1996, and SPAWC in 1997) and guest (co-) edited four special issues. He has served as an Associate Editor for the IEEE TRANSACTIONS ON SIGNAL PROCESSING and the IEEE SIGNAL PROCESSING LETTERS. He is a secretary of the SP Conference Board, a member of the SP Publications Board and a member and Vice-Chair of the Statistical Signal and Array Processing Committee. He is a member of the Editorial Board for the PROCEEDINGS OF THE IEEE, he chairs the SP for Communications Technical Committee and serves as the Editor-in-Chief for the IEEE SIGNAL PROCESSING LETTERS. He is a member of the IEEE Fellows Election Committee, the IEEE-SP Society's Board of Governors, and a frequent consultant for the telecommunications industry.